Application Report
SBOA114–February 2006

Design Methodology for MFB Filters in ADC Interface Applications

Michael Steffes *High-Speed Products*

ABSTRACT

While the Multiple FeedBack (MFB) filter topology is well-known, its application to very high dynamic range analog-to-digital converter (ADC) interfaces requires a careful consideration of component value selection. This application report develops the ideal transfer function, then introduces a component selection methodology and discusses its impact on noise and distortion. The impact of amplifier Gain Bandwidth Product on final pole locations is also included, showing several examples. A complete high dynamic range, differential I/O filter for wide dynamic range ADC driving is then designed. A simple design spreadsheet embodying this design approach is available for download with this application report.

Contents

List of Figures

1 MFB Filter Transfer Function

The Multiple FeedBack (MFB) filter is widely used for very high dynamic range ADC input stages. This filter offers exceptional stop band rejection over other filter topologies (Ref. 1). Figure 1 shows the starting point for this filter design.

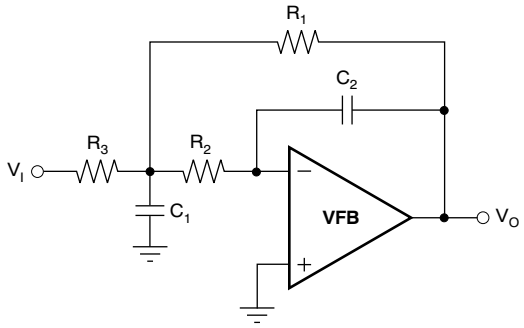

Figure 1. MFB Filter Topology

This design is an inverting signal path, 2nd-order, low-pass filter that offers numerous advantages over Sallen-Key filters. This single-ended I/O interface can be easily adapted to a differential I/O interface, as will be shown later.

A few of the advantages of this topology include:

1. No gain for the noninverting current noise and/or DC bias current. Figure 1 shows the non-inverting input grounded, which is great for reducing noise but less than ideal for DC precision. Adding a resistor equal to the DC impedance looking out the inverting node achieves bias current cancellation; adding a capacitor across this resistor reduces the noise contribution for the resistor and the op amp bias current noise. If the amplifier is a JFET or CMOS type, this bias current cancellation will not work and the noninverting input should simply be set to ground or a desired reference voltage.
2. The in-band signal gain is set by $-(R_1/R_3)$. As will be shown, R_3 also sets the Q of the filter while having no influence over ω_o.

Embedded within the filter is an Integrator comprised of R_2 and C_2, along with the Voltage FeedBack (VFB) op amp. This design normally needs to be implemented using a unity-gain stable, VFB op amp because the core gain element needs to be configured as an Integrator. There are dynamic range advantages to using non-unity-gain stable VFB amplifiers and a design approach for successfully applying those types of devices will be shown later. However, a Current FeedBack (CFB) op amp is usually not suitable to this type of filter since its local stability requires a feedback resistor nearly equal to a recommended value. A capacitive feedback as required in Figure 1 will typically not work with CFB amps without some design tricks that usually impair noise performance (Ref. 2). Since the emerging Fully Differential Amplifiers (FDA) are essentially voltage feedback op amps, they can also be applied quite successfully to this topology (Ref. 3).

Numerous approaches to selecting the component values are available in the literature (see, for example, Ref. 4). An equal-R approach is common, and will be shown as a desirable approach once an initial R_2 is chosen. As ADCs continue to improve, the resistor noise in this filter can actually be a dominant element in the total noise spectrum delivered to the converter input. One outcome of the equal-R design (Ref. 4) is that quite unequal Cs are then required for most filter targets. That is in fact generally true for this filter type (as will be shown later). If an equal C design is desired, another filter type should be considered (Sallen-Key).

The Laplace transfer function for the circuit of Figure 1 is shown as Equation 1.

$$\frac{V_o}{V_i} = \frac{-1}{C_1C_2R_2R_3} \cdot \frac{1}{s^2 + s\frac{1}{C_1R_2R_3}\left(R_3 + R_2\left(1 + \frac{R_3}{R_1}\right)\right) + \frac{1}{R_1R_2C_1C_2}} \tag{1}$$

The various design goals of interest in this equation can be solved as:

- the DC gain (where *s* = 0):

$$A_V(DC) = -\frac{R_1}{R_3} \quad [\text{in V/V}] \tag{2}$$

- characteristic frequency:

$$\omega_o = \sqrt{\frac{1}{R_1R_2C_1C_2}} \quad [\text{in radians}] \tag{3}$$

- the quality factor:

$$Q = \frac{\sqrt{\frac{C_1}{C_2}}}{\sqrt{\frac{R_1}{R_2}} + \sqrt{\frac{R_2}{R_1}} + \frac{\sqrt{R_1R_2}}{R_3}} \quad [\text{unitless}] \tag{4}$$

Or, with $\alpha \equiv \frac{R_1}{R_2}$,

$$Q = \frac{R_3\sqrt{\frac{C_1}{C_2}}}{R_2\sqrt{\alpha} + R_3\left(\sqrt{\alpha} + \frac{1}{\sqrt{\alpha}}\right)} \tag{5}$$

As is usually the case in active filter design, there are more passive elements to be resolved than filter characteristics. Here, there are five elements and only three targets. This situation often leads to the very common equal-R assumption to reach a design where that is a somewhat arbitrary way to eliminate one degree of freedom. There should be a more rational way to select component values for these filters.

Looking at the circuit of Figure 1 at DC gives the simplified circuit of Figure 2 that will be used to show the DC part of the low-pass filter.

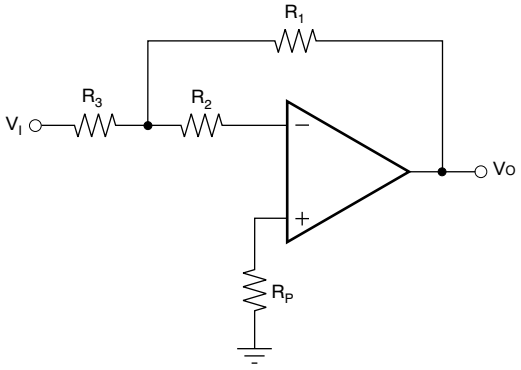

Set: $R_P = R_2 + R_1 \quad R_3$

Figure 2. DC Analysis Circuit

A resistor (R_P) has been added on the noninverting input to provide for DC bias current cancellation in the output offset voltage. Setting it as shown reduces the output DC error to ($I_{OS} \bullet R_1$) if the op amp shows an input bias current that has an offset current specification. Again, JFET or CMOS amplifiers would not use this R_P resistor for output DC error reduction.

The total output noise is a considerably more involved discussion. Appendix A develops that expression for the circuit of Figure 2, where the bandlimiting effects of the filter capacitors are neglected. The total output noise is given as Equation 6 (which is also Equation A-3 in Appendix A), where the terms arising from R_P are neglected.

$$e_o = \sqrt{(e_n)^2\left(1+\frac{R_1}{R_3}\right)^2 + 4kTR_2\left(1+\frac{R_1}{R_3}\right)^2 + 4kTR_1\left(1+\frac{R_1}{R_3}\right) + {i_n}^2\left[R_2\left(1+\frac{R_1}{R_3}\right)+R_1\right]^2} \tag{6}$$

It would be reasonable to assume that most designs would not want the resistor terms to add too much more noise at the output than the op amp noise voltage itself. This idea can be used to develop Equation 7 (Equation A-4 in Appendix A) where the op amp noise voltage (squared) is targeted to be equal to the total noise power contribution of the R_2 and R_3 resistors at the output.

$$\left(1+\frac{R_1}{R_3}\right)^2 {e_n}^2 = \left(4kTR_2 + \left(i_nR_2\right)^2\right)\left(1+\frac{R_1}{R_3}\right)^2 + {i_n}^2\left(2R_2R_1\left(1+\frac{R_1}{R_3}\right)\right) \tag{7}$$

This expression still includes both R_1 and R_3. R_3 is also a resistor that will contribute to the total output noise in a similar fashion to R_2. It would be preferable to make it as low as possible within the constraint that it should not load the driving signal source to the point of creating a dominant distortion mechanism in that prior stage. As a maximum value, it might be reasonable to let it equal R_2 while recognizing that moving it lower will benefit the total output noise. If R_3 is tentatively set equal to R_2, Equation 7 can be simplified and put into a form to solve for R_2, as shown in Equation 8 (from Equation A-13 in Appendix A).

$${R_2}^2 + R_2\left(\frac{1+A_V}{1+3A_V}\right)\frac{4kT}{({i_n}^2)} - \left(\frac{1+A_V}{1+3A_V}\right)\left(\frac{e_n}{i_n}\right)^2 = 0 \tag{8}$$

This equation may then be solved using the quadratic equation for an initial target value for R_2 as shown in Equation 9 (where only the positive solution for R_2 is used; note that Equation 9 is also Equation A-14 in Appendix A).

$$R_2 = \left(\frac{1+A_V}{1+3A_V}\right)\frac{2kT}{({i_n}^2)}\left[\sqrt{1+\left(\frac{1+3A_V}{1+A_V}\right)\left(\frac{e_n}{2kT}\right)^2} - 1\right] \tag{9}$$

This formula gives an initial suggested value for R_2 (note that embedded in this solution is the assumption that R_3 will then be set equal to R_2). Both R_2 and R_3 may be set lower to improve noise. Recognize, however, that very low values will start to load the output stage driving into this filter and the filter op amp output stage (if R_1 is also very low). They can also be set higher to lighten the loading where an increase in total output noise will be the result.

Once R_2 is selected, either from this noise consideration or from some other approach, we now need to select one of the capacitor values to remove it from the filter design equations. With two elements selected, the remaining three can be used to set the three filter design goals. In solving to achieve the desired filter shape, it is possible (Appendix B) to arrive at an equation for C_1 that shows a critical constraint on the R_2C_2 product. That constraint can be seen in Equation 10 (which is taken from Appendix B as Equation B-22):

$$C_1 = \frac{Q}{\omega_o R_2\left(1 - Q\omega_o R_2 C_2\left(1+A_V\right)\right)} \tag{10}$$

Equation 10 clearly shows that the R_2C_2 product must be low enough to keep the solution for $C_1 > 0$. That constraint is shown as Equation 11:

$$\omega_o R_2 C_2 < \frac{1}{Q\left(1+A_V\right)} \quad \text{for } C_1 > 0 \tag{11}$$

or:

$$\frac{1}{\omega_o R_2 C_2} > Q\left(1+A_V\right) \quad \text{[ratio of Integrator pole to target } \omega_o\text{]} \tag{12}$$

($1 / \omega_o R_2 C_2$) is physically the ratio of the Integrator pole to the target ω_o. Equation 12 sets a minimum limit for that ratio, while moving above that limit is essentially moving the Integrator pole out relative to ω_o (reducing C_2 if ω_o and R_2 are fixed). Solving for equality in Equation 12 solves for an infinite value of C_1. So, moving the Integrator pole out also reduces the required value for C_1 from infinity to some more reasonable value.

While Equation 11 and Equation 12 give a nice limit on a solution for C_2 and C_1 (note that once C_2 is selected, Equation 10 gives C_1 completely defined by the desired filter shape and a selected R_2 value), they do not tell us much about where to place the Integrator pole.

One option considered for many active filter designs is to set the two capacitors equal. This solution is sometimes considered preferable to get better matching in order to minimize the sensitivity functions. Equation 10 actually gives us an easy way to test this approach by temporarily targeting $C_1 = C_2$, then solving the resulting expression for C_2 (Appendix C). Equation 13 shows the resulting quadratic while Equation 14 shows the solution for C_2. Again, this simplified approach is only possible if R_2 is initially selected from either a noise approach or some other consideration.

$$C_2^2 - C_2 \frac{1}{R_2 Q \omega_o (1 + A_V)} + \frac{1}{(R_2 \omega_o)^2 (1 + A_V)} = 0 \tag{13}$$

(which is Equation C-3 in Appendix C;)

$$C_2 = \frac{1}{2 Q R_2 \omega_o (1 + A_V)} \left(1 \pm \sqrt{1 - (2Q)^2 (1 + A_V)} \right) \tag{14}$$

(which is Equation C-10 in Appendix C;)

The radical in Equation 14 only solves for non-imaginary C_2 values if $(2Q)^2 \bullet (1 + A_V) \leq 1$. Assuming a minimum $A_V = 1$ requires a $Q < 0.353$. Setting $Q = 0.353$ and $A_V = 1$ gives a C_2 solution that is two repeated values given in Equation 15:

$$C_2 = C_1 = \frac{1}{1.43 R_2 \omega_o} \tag{15}$$

Using an active filter for a $Q < 0.5$ (two real poles) and/or gain < 1 is unlikely because a simple passive circuit can easily provide attenuation and two real poles without requiring an active element. Thus, an equal C design is interesting but not particularly useful for an MFB filter design.

2 MFB Active Filter Noise Gain Analysis

One possible approach to setting the ($1 / R_2 C_2$) product (Integrator pole location) is to investigate what impact it might have on the resulting noise gain for the completed filter. Recall that the noise gain is the reciprocal of the feedback attenuation from the op amp output pin back to the inverting input pin. This noise gain is an important consideration for at least three reasons.

1. Any peaking in the noise gain will, of course, peak up the gain to the output for the total equivalent input voltage noise (including the R_2 effects considered earlier).
2. Noise gain peaking will also reduce the loop gain. All other things being equal, reduced loop gain will show up as higher output harmonic distortion.
3. The point where the noise gain crosses the open-loop gain (in a Bode plot) also determines the loop gain phase margin. Phase margin at this crossover point sets the stability for the overall design.

The feedback divider circuit for the MFB filter is shown in Figure 3. An added element is included here that was not in Figure 1—a parasitic or intentional capacitor (C_T) on the inverting input pin.

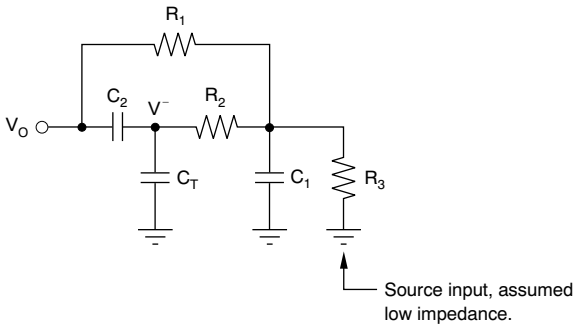

Figure 3. Feedback Analysis Circuit for MFB Filter

Here, it is easy to see the *multiple feedback* nature of the circuit. At DC, the path is through R_1 and R_2, while at high frequencies it is through C_2.

The desired Laplace transfer function here is from V_O to V^- (the inverting input voltage). This attenuator is normally referred to as the β in control theory discussions of negative feedback systems. The solution for β is shown as Equation 16.

$$\beta \equiv \frac{V^-}{V_O} = \frac{C_2}{C_T + C_2} \cdot \frac{s^2 + s\left[\frac{1}{C_1R_3} + \frac{1}{C_1(R_1 \| R_2)}\right] + \frac{1}{R_1R_2C_1C_2}}{s^2 + s\left[\frac{1}{C_1R_3} + \frac{1}{C_1(R_1 \| R_2)} + \frac{1}{R_2(C_T + C_2)}\right] + \frac{1}{R_2(R_1 \| R_3)C_1(C_T + C_2)}} \tag{16}$$

We are normally more interested in looking at 1 / β, which will be the noise gain discussed earlier.

Inverting Equation 16 gives Equation 17.

$$\frac{1}{\beta} = \left(1 + \frac{C_T}{C_2}\right) \cdot \frac{s^2 + s\left[\frac{1}{C_1R_3} + \frac{1}{C_1(R_1 \| R_2)} + \frac{1}{R_2(C_T + C_2)}\right] + \frac{1}{R_2(R_1 \| R_3)C_1(C_T + C_2)}}{s^2 + s\left[\frac{1}{C_1R_3} + \frac{1}{C_1(R_1 \| R_2)}\right] + \frac{1}{R_1R_2C_1C_2}} \tag{17}$$

There are several key points to Equation 17:

1. The poles are identical to the desired filter poles.
2. The DC ($s = 0$) gain becomes $(1 + R_1/R_3)$.
3. The high frequency gain (as $s \rightarrow \infty$) goes to $(1 + C_T/C_2)$.
4. If $C_T << C_2$, then the high frequency noise gain approaches 1.

The noise gain transfer function has two zeroes and two poles. The transition between the DC gain and high frequency gain depends on the relative position of the zeroes and poles. It would be preferable to minimize the peaking in the noise gain within the desired low-pass frequency band as it makes this transition from the DC gain to the $s \rightarrow \infty$ gain. If the desired filter shape calls for a high Q, peaking in this noise gain response is unavoidable as the frequency approaches ω_o. If, however, one or both zeroes are placed to fall below the ω_o frequency, added noise gain peaking results that might be unnecessary. The question then is whether or not those zeroes can be placed above ω_o in order to limit any additional ***in-band*** peaking for the noise gain.

Starting from Equation 17, first set $C_T = 0$ for this portion of the analysis. It will be used later to allow non-unity-gain stable amplifiers to be used in the MFB topology, but will unnecessarily complicate the resolution of $(1 / R_2C_2)$. Rewriting Equation 17 with this simplification yields Equation 18.

$$\frac{1}{\beta} = \frac{s^2 + s\left[\frac{1}{C_1R_3} + \frac{1}{C_1(R_1 \| R_2)} + \frac{1}{R_2C_2}\right] + \frac{1}{R_2(R_1 \| R_3)C_1C_2}}{s^2 + s\left[\frac{1}{C_1R_3} + \frac{1}{C_1(R_1 \| R_2)}\right] + \frac{1}{R_1R_2C_1C_2}} \tag{18}$$

Then, observing that the numerator coefficients are very nearly the same as the denominator coefficients, we can rewrite the noise gain equation in terms of the desired filter characteristics as shown in Equation 19.

$$\frac{1}{\beta} = \frac{s^2 + s\left[\frac{\omega_o}{Q} + \frac{1}{R_2C_2}\right] + (1 + A_V)\omega_o{}^2}{s^2 + s\left[\frac{\omega_o}{Q}\right] + \omega_o{}^2} \qquad \text{[MFB noise gain]} \tag{19}$$

Here, it becomes very apparent that the embedded Integrator pole location, $(1 / R_2C_2)$, is the one added degree of freedom in setting the noise gain zeroes. All of the other elements feeding into the noise gain zero coefficients are set by the desired low-pass, 2nd-order filter terms. It is therefore very useful to cast the design analysis in terms of this Integrator pole location. More specifically, working in terms of the ratio $(1 / \omega_o R_2C_2)$ allows better simplification and is simply the ratio of the target characteristic frequency and the embedded Integrator pole location.

3 Setting the Integrator Pole to Improve Noise and Distortion

One limit to the range on $(1 / \omega_o R_2C_2)$ has already been set in Equation 12 to achieve real values for C_1. Setting $(1 / \omega_o R_2C_2)$ equal to $Q\ (1 + A_V)$ will solve C_1 for infinity and R_3 for zero. Neither of these values are particularly useful for implementation, but are interesting as a limit to the noise gain zero locations. Using Equation 12 to set a minimum level for $1 / R_2C_2$ gives $\omega_o \bullet Q \bullet (1 + A_V)$. Putting this result into the numerator of Equation 19, and solving for the equivalent Q_C for the zeroes of the noise gain in terms of the desired filter shape terms, gives Equation 20 (from Appendix D, Equation D-9).

$$Q_C = \frac{Q\sqrt{1 + A_V}}{1 + Q^2(1 + A_V)} = \frac{x}{1 + x^2} \qquad [\text{where } x = Q\sqrt{1 + A_V}\ ] \tag{20}$$

This result is very useful in that it clearly shows the maximum possible value for Q_C is one-half. (1) This occurs for any combination of desired A_V and Q that sets $Q \bullet \sqrt{(1 + Av)} = 1$. The most common condition for this would be Q = 0.707 (Butterworth target) and $A_V = 2$. That combination, with a target for the Integrator pole set by Equation 12, gives repeated real zeroes at ω_o / Q (Appendix D). Several important conclusions come from this combination.

1. The noise gain zeroes are always two real zeroes.
2. They are repeated, and at the maximum value, at ω_o / Q for the specific conditions described above (which is not realizable since $C_1 = \infty$).
3. For Q > 1, it will necessarily be the case that one of the zeroes will fall below the target ω_o. This observation says that higher Q targets in the MFB filter have an added peaking in the noise gain beyond just the desired filter pole peaking because one of the noise gain zeroes moves below ω_o.
4. Moving the target $(1 / \omega_o R_2C_2)$ up (moving the Integrator pole out) to get a real solution for C_1 effectively moves one of the zeroes up in frequency and the other down in frequency along the negative real axis in the *s*-plane.
5. It turns out that this higher zero location corresponds very closely to $1 / R_2C_2$ as the zeroes become widely separated.

As the $(1 / \omega_o R_2C_2)$ target is increased from its minimum of $Q \bullet (1 + A_V)$, C_1 comes down from infinity and R_3 increases from zero. These changes are both desirable within some limits. As R_3 starts to increase beyond the targeted R_2 value (from the noise analysis of Equation 9), it will also start to add meaningfully to the total output noise. One possible limit to R_3 is to set it equal to R_2 and resolve what this means for a $(1 / \omega_o R_2C_2)$ target. Equation 21 shows this result (from Appendix E).

$$\frac{1}{\omega_o R_2C_2} = Q(2A_V + 1) \qquad [\text{where } R_3 = R_2 \text{ is desired}] \tag{21}$$

Appendix E goes on to solve for the resulting zero location if Equation 21 is used to set $1 / R_2C_2$. That result is shown as Equation 22 (Equation E-16 from Appendix E).

$$Z_{1,2} = -\frac{\omega_o}{2Q}\left(1 + Q^2(2A_V + 1)\right)\left[1 \pm \sqrt{1 - \left(\frac{2Q\sqrt{1 + A_V}}{1 + Q^2(2A_V + 1)}\right)^2}\right] \tag{22}$$

(1) $x / (1 + x^2)$ reaches a maximum value equal to 1/2 over $0 \le x \le \infty$ at x = 1.

Setting 1 / R_2C_2 as given in Equation 21 gets $R_3 = R_2$. It also sets the two noise gain zeroes as given by Equation 22. Moving the target (1 / $\omega_o R_2 C_2$) below the value set by Equation 21 pulls the Integrator pole down, moves the lower zero to a higher frequency (acting to reduce the noise gain peaking), and reduces R_3 below R_2. All of these desirable effects suggest that (1 / $\omega_o R_2 C_2$) should be set slightly below the value determined by Equation 21 as long as the resulting R_3 is not so low as to present too heavy a load for the driving source into the filter. Since R_3 in Figure 1 looks into a virtual ground node *in-band*, the input impedance below cutoff will be R_3. Conversely, moving the (1 / $\omega_o R_2 C_2$) above the value set by Equation 21 increases R_3 beyond the targeted R_2 value, moves the lower noise gain zero down further (causing added peaking in the noise gain within the desired frequency passband), and extends the higher noise gain zero out in frequency (approximating the 1 / R_2C_2 Integrator pole location).

In summary, the (1 / $\omega_o R_2 C_2$) target should be set within the range indicated in Equation 23.

$$Q(A_V + 1) \; < \; \frac{1}{\omega_o R_2 C_2} \; \leq \; Q(2A_V + 1) \tag{23}$$

Setting $\frac{1}{R_2 C_2} = \omega_o Q(2A_V + 1)$ gives $R_3 = R_2$

while setting $\frac{1}{R_2 C_2} = \omega_o Q(A_V + 1)$ gives $C_1 \rightarrow \infty$ and $R_3 = 0$ (24)

4 Example Designs Showing the Impact of Integrator Pole Location

Now let's use these results to step through a design and observe the noise and distortion that results from various selections of (1 / $\omega_o R_2 C_2$). All of these designs give the desired filter shape. It is the noise gain shape and noise contributions of the resistor values that are of interest here.

Start with a target design given by:

- $\omega_o = 2\pi \bullet 1\text{MHz}$
- Q = 0.707
- A_V = 2 (gives a negative gain of 2 for the signal path)

Then, pick an amplifier to get its noise and open-loop gain characteristic. For this first example, we will use the single channel OPA820—a relatively low-noise, unity-gain stable, wideband VFB op amp. The necessary specifications for this part of the design are shown in Table 1.

Table 1. OPA820 Noise and Open-Loop Gain Specifications

PART NO.	GBW (MHz)	e_n (nV/$\sqrt{\text{Hz}}$)	A_{OL} (V/V)	i_n (pA/$\sqrt{\text{Hz}}$)
OPA820	280	2.5	2000	1.7

The targeted maximum R_2 value is calculated using Equation 9, giving this result:

- Suggested R_2 = 366.38Ω

Picking R_2 = 250Ω will allow us to proceed to setting the (1 / $\omega_o R_2 C_2$) target. The recommended range (using Equation 23) is:

- Minimum allowed ratio of Integrator/ω_o pole is: **2.12**
  - This result sets a limit to getting a valid solution for C_1
- Maximum value to get $R_3 = R_2$ is: **3.53**
  - This result sets $R_3 = R_2$ for noise control

If the $R_3 = R_2$ value is chosen, the resulting zero locations are (from Equation 22):

- First, compute the radical for the polynomial: **0.714241334**
  - The lower zero location is **707kHz**
  - The upper zero location is **4.24MHz**

Continuing with the $R_3 = R_2$ solution, the final component values to place into Figure 1 and the design sequence are:

- R_2 = **250Ω** [selected to control noise using Equation 9]
- C_2 = **180pF** [set by targeting $(1 / \omega_0 R_2 C_2) = Q(2A_V + 1)$]
- C_1 = **1130pF** [set using Equation 10]
- R_3 = **250Ω** [set using Equation B-17]
- R_1 = **500Ω** [set using Equation 2]
- DC Gain (A_V) = **2.00V/V** [from Equation 2]
- F_O = **1MHz** = F_{-3dB} (if Q = 0.707) [from Equation 3]
- Q = **0.707** [from Equation 4]

The noise gain and phase can be computed using Equation 17 where C_T = 3pF is used to emulate a parasitic capacitance on the inverting op amp input. This noise gain and phase can be plotted along with the open-loop gain and phase for the OPA820. Finally, the phase margin where this noise gain intersects the open-loop response can be derived.

The example circuit developed here is shown as Figure 4.

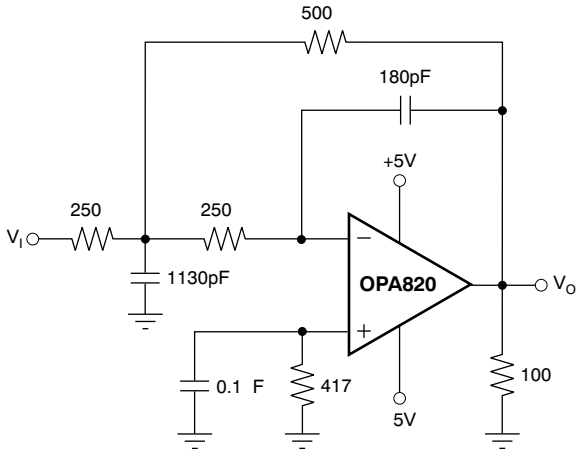

Figure 4. Initial Test Circuit using the OPA820 in a 1MHz, Butterworth Low-Pass Filter Configuration

This circuit gives the loop gain plot of Figure 5.

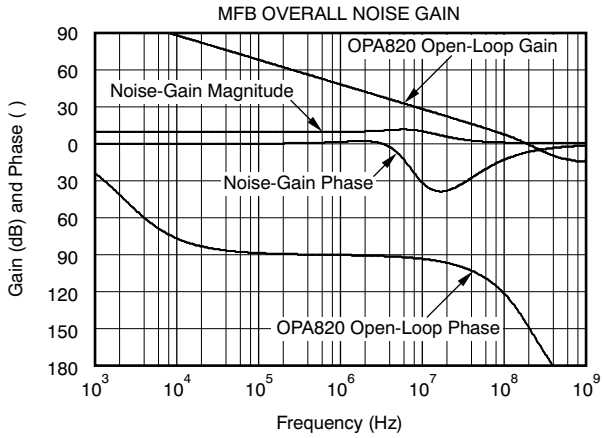

Figure 5. Noise Gain and Open-Loop Gain for Circuit in Figure 4

This plot transitions fairly smoothly from a noise gain of 20log(3) = 9.5dB to 0dB with only minor peaking as a result of the noise gain zero at 707kHz. Phase margin for this circuit is 51 degrees, which is quite stable.

In order to test the impact of setting the $(1 / \omega_0 R_2 C_2)$ target far too high, set it to 10 and repeat the design in this manner (still holding $R_2 = 250\Omega$):

- R_2 = **250Ω** [selected to control noise using Equation 9]
- C_2 = **63.7pF** [set by targeting $(1 / \omega_0 R_2 C_2) = 10$]
- C_1 = **571pF** [set using Equation 10]
- R_3 = **1.39kΩ** [set using Equation B-17]
- R_1 = **2.79kΩ** [set using Equation 2]
- DC Gain (A_V) = **2.00V/V** [from Equation 2]
- F_O = **1MHz** [from Equation 3]
- Q = **0.707** [from Equation 4]

Figure 6 shows the new design circuit with these more widely separated noise gain zeroes (these zeroes are now at 268kHz and 10.7MHz, solving the numerator of Equation 19).

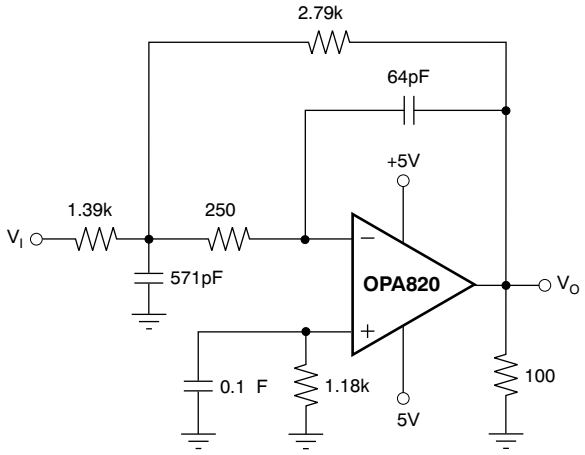

Figure 6. New Design Circuit with Noise Gain Peaking

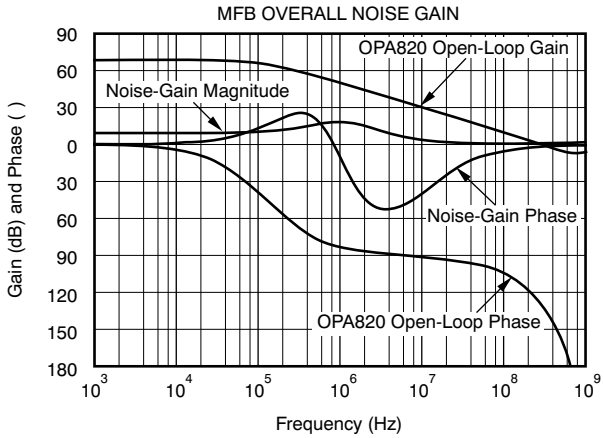

Figure 7. Noise Gain Plot for Figure 6

The loop phase margin is not impacted greatly, going to 54 degrees. This value is slightly better than the previous one, and still very stable. The plot of Figure 7 clearly shows this lower zero in the phase response. The noise gain phase curve peaks up much more as the zero comes in earlier and before the two poles reverse it. More importantly, the noise gain peaks up slightly, reducing the available loop gain in the passband.

Both design points give the same desired filter shape. Figure 8 shows the simulated small signal frequency response for both sets of filter component values. Figure 8 shows the desired maximally flat response with a 1MHz cutoff.

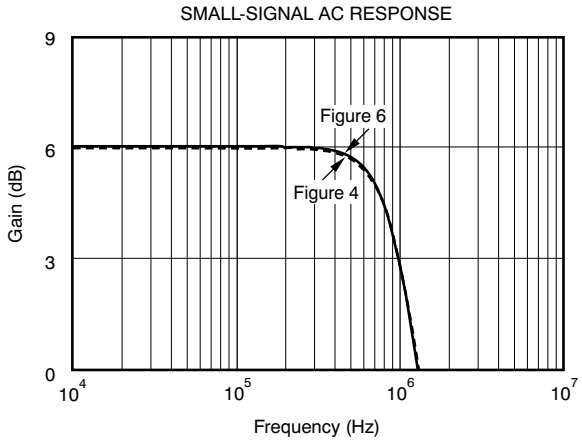

Figure 8. Simulated Small Signal Bandwidth for Figure 4 and Figure 6

Consider the impact of the different loop gains. Assume this circuit was intended for very low distortion through 600kHz. The loop gain at 600kHz for Figure 5 is 42.8dB while that of Figure 7 is 37.4dB. The 5.4dB loss in loop gain as a result of noise peaking should show up directly in harmonic distortion. Simulating each circuit for 3rd-harmonic (recognizing that harmonic is falling on the filter skirt at 1.8MHz) gives the results shown in Table 2. This simulation was looking at the 3rd-harmonic since that term has shown good correlation to measured data (while even-order terms do not correlate well from simulation to bench measurements) . Also, a 100Ω load with a $2V_{PP}$ output was intentionally used to bring the distortion terms up from very low levels. A lighter load (such as an ADC input) will have much lower distortion than reported in this example.

Table 2. Results of 3rd-Harmonic Simulation at 600kHz, $V_O = 2V_{PP}$, $R_L = 100\Omega$

TEST CIRCUIT	HD3 (dBc)
Figure 4	–83.9
Figure 6	–78.7

The different noise gain shapes have indeed produced a 5.2dB drop in distortion performance—very nearly equal to the predicted 5.4dB drop from the difference in loop gains at 600kHz.

Figure 7, with the higher resistor values and peaked noise gain, also gives a higher output noise for the circuit shown in Figure 6 as compared to that of Figure 4. Figure 9 plots the output spot noise over frequency for both circuits. This simulation includes every noise source both inside the amplifier and the external resistors. A portion of the low frequency noise (that is decreasing from a high value at 100Hz) comes from the bias current cancellation resistor on the noninverting input pin. That noise is rolled off by the 0.1µF capacitor to show the low frequency shape in Figure 9. Part of that higher low frequency noise is also the 1/f noise modeled by the OPA820.

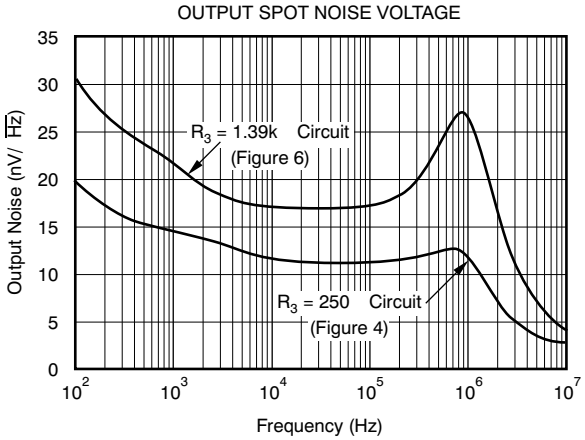

Figure 9. Output Spot Noise Comparison

As expected, the second design point with the peaked noise gain (and much higher R_3 value) shows significantly higher output noise and more peaking. This noise integrates to considerably higher output V_{PP} noise over the design of Figure 4.

5 MFB Filter Implemented with Non-Unity-Gain Stable Op Amps

Non-unity-gain stable VFB op amps offer numerous advantages for very high dynamic range applications. Most of these devices offer lower noise, higher slew rate, and higher open-loop gain over similar unity-gain stable compensated versions. For the very lowest distortion and noise, it would be desirable to apply these devices in this MFB filter application. However, since the basic MFB circuit shapes the noise gain to be a unity gain feedback at high frequencies, a bit of additional work is needed in order to take advantage of the intrinsically higher dynamic range offered by these devices.

As an example, use the non-unity-gain stable OPA2614 (a dual) to implement a 3rd-order Bessel filter at 5MHz. The OPA2614 (290MHz gain bandwidth product, or GBW) has a unity-gain stable version, the OPA2613 (125MHz GBW), that could also be used here. In this case, the noise numbers of the two versions are identical, but the higher gain bandwidth will give 20Log(290/125) = 7.3dB more loop gain at any frequency above the dominant open-loop pole. This design is working towards a single +5V supply, differential-in-to-differential-out, gain of 2 interface that includes this 3rd-order linear phase filter. The real pole is implemented as the RC filter that often appears between the amplifier and the ADC.

First, we must find the required pole locations for this filter. Setting up the design targets in FilterPro™ (Ref. 5) for a 3rd-order Bessell with 5MHz cutoff gives the following required pole location. (**Note**: FilterPro also gives simplified circuit designs, but we are only using the pole calculation feature from FilterPro and will use the circuit design tools developed in this application note to select component values.)

- Real pole at 5.76MHz
- Complex poles F_O = 7.24MHz
- Q = 0.691

Stepping through the single amplifier design using the OPA2614 data, we first need a target R_2 as shown in Table 3.

Table 3. OPA2614 Calculations for Target R_2

PART NO.	GBW (MHz)	e_n (nV/√Hz)	A_{OL} (V/V)	i_n (pA/√Hz)
OPA2614	290	1.8	70,800	1.7
Suggested R_2 = 195.59Ω		This is solving for R_2 noise less than op amp noise using Equation 9.		
We pick **R_2 = 200Ω**		**Note:** R_2 could be greater than this, but probably not too much in order to limit output noise.		

Then we perform the calculation for the limits on the $(1 / \omega_0 R_2 C_2)$ target:

- Minimum allowed ratio of Integrator pole/ω_0 is: **2.07**
  - This gives a solution for $C_1 = \infty$
- Maximum value to get $R_3 = R_2$ is: **3.45**
  - This result sets $R_3 = R_2$ for noise control

Use the 3.45 target to get $R_3 = R_2$.

Then the completed design can be summarized with these component values:

- R_2 = **200Ω** [selected to control noise using Equation 9]
- C_2 = **31.8pF** [set by targeting $(1 / \omega_0 R_2 C_2) = Q(2A_V + 1)$]
- C_1 = **189pF** [set using Equation 10]
- R_3 = **201Ω** [set using Equation B-17]
- R_1 = **402Ω** [set using Equation 2]
- DC Gain (A_V) = **2.00V/V** [from Equation 2]
- F_O = **7.24MHz** [from Equation 3]
- Q = **0.691** [from Equation 4]

The completed 3rd-order filter design is shown in Figure 14, where a differential implementation is illustrated.

Lastly, going into the loop gain analysis with C_T = 3pF initially gives noise gain zeroes at 5MHz and 28MHz, with the Bode plot for the open-loop and noise gain and phase shown in Figure 10.

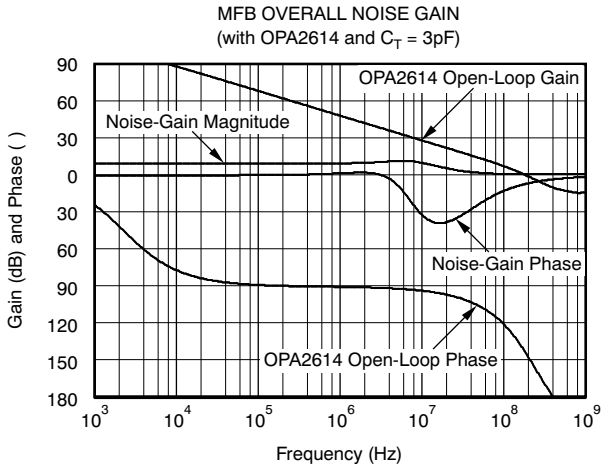

Figure 10. Noise Gain Plot for Initial OPA2614 MFB Filter Design

This analysis shows a phase margin equal to 33 degrees. While this phase margin is still stable, some peaking around 200MHz might be expected in the small signal response. Often, this low degree of phase margin also has more part-to-part and temperature variation in that peaking. As noted earlier, the noise gain can be raised at high frequencies by adding C_T on the inverting node. Targeting a gain of 2 at high frequencies requires $C_T = C_2$ = 31.8pF. Re-running the loop gain analysis with C_T = 31.8pf gives noise gain zeroes at 4.2MHz and 19MHz, with the Bode plot shown in Figure 11.

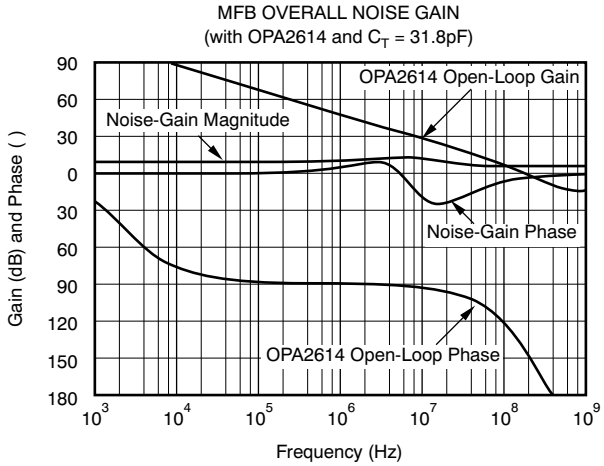

Figure 11. Noise Gain with OPA2614 Open-Loop Gain for C_T = 31.8pF

This plot clearly shows that the crossover (the point where the noise gain crosses the open-loop gain) has dropped back to 100MHz. This results in an improved phase margin of 52 degrees—which is considerably more design margin to avoid unnecessary peaking or oscillation.

The desired signal frequency response is achieved using either design. Figure 12 (C_T = 3pF or 31.8pF) illustrates the expanded plot around cutoff for either design, showing both the output pin response and the final targeted response at C_{LOAD} in Figure 14. Both designs hit the desired 5MHz cutoff.

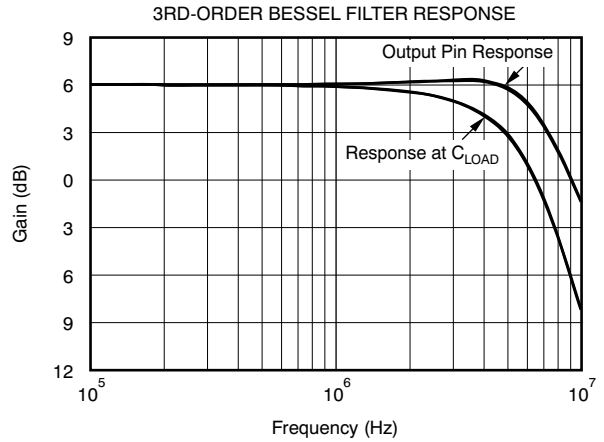

Figure 12. Frequency Response for the OPA2614 MFB Filter Design (Each 1/2 of Figure 14)

Expanding this plot to show the detail at 200MHz exposes the slight peaking caused by the low phase margin in the C_T = 3pF design (see Figure 13). Adding the C_T = 31.8pF smooths this peaking out quite a bit, with minimal change in the overall response. This basic technique is even more important if higher minimum stable gain amplifiers are applied to this circuit (such as the OPA2846).

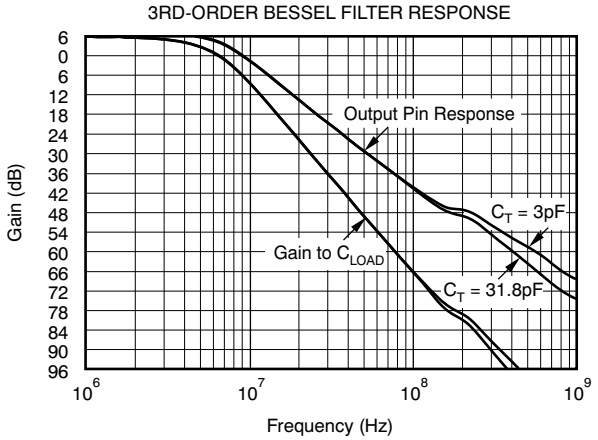

Figure 13. Expanded View of 3rd-Order Filter Response (see Figure 14)

Figure 13 also shows one of the advantages of the MFB filter followed by a simple RC as part of a 3rd-order design. This approach gives very good stop band rejection to very high frequencies. Other filter approaches (for example, the Sallen-Key) show an increasing gain at very high frequencies as a result of 2nd-order effects (Ref. 1).

6 Differential Version of 3rd-Order Design

One very useful application for the MFB filter design is providing a single-supply differential interface to high-performance ADCs with very low distortion and noise. The OPA2614 design can be easily adapted to this requirement. One new issue is to provide a midsupply DC bias at the noninverting input to keep the signal swing centered between the supplies. Sometimes, this can be provided as the V_{CM} from the ADC. Alternatively, a voltage divider from the supply can be used. If the best output DC precision is desired, the source impedance looking out of each noninverting input should again match the total DC impedance looking out of the inverting input of each channel as described in Figure 2. Figure 14 shows the differential implementation for the 3rd-order filter designed previously. Here, separate noninverting bias resistors from V_{CM} are used. If DC precision is a secondary concern, a single bias resistor (or resistor divider from the supply) could also be used.

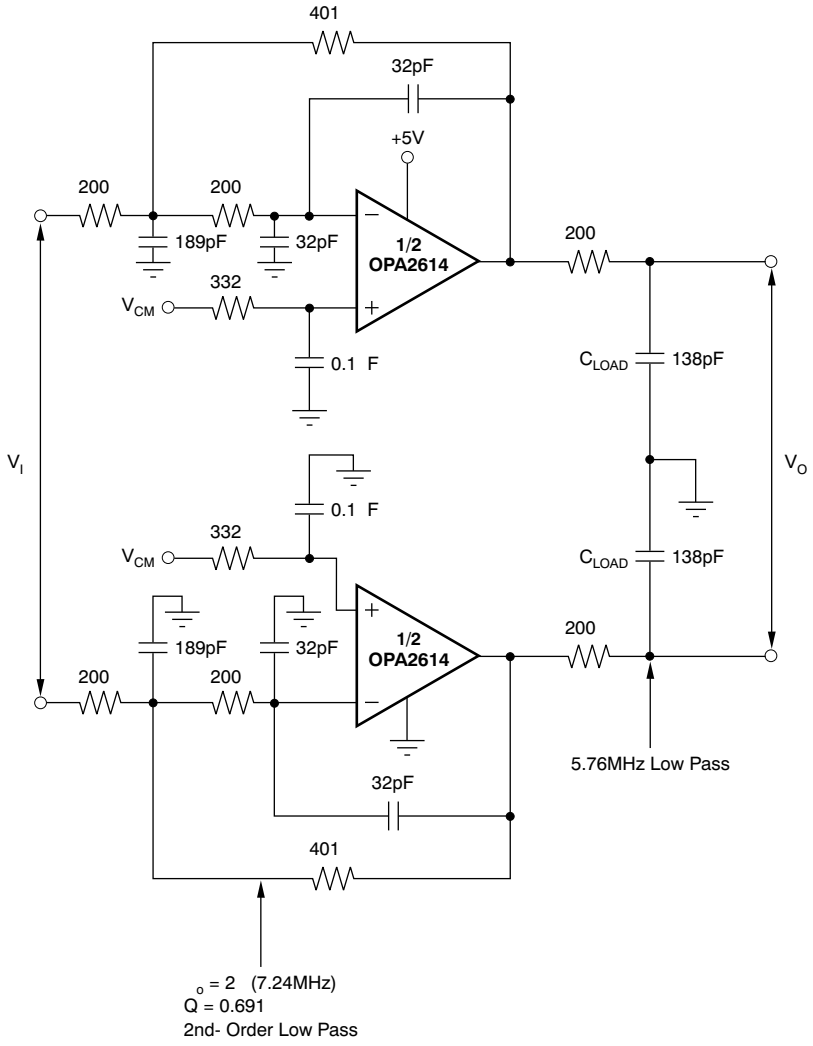

Figure 14. Single-Supply Differential ADC Interface with 3rd-Order Bessel Filter (with f_{-3dB} = 5MHz)

The overall filter shape is that shown in Figure 13—a 3rd-order Bessel with a 5MHz cutoff. One critical implementation choice made in Figure 14 is to keep separate grounded capacitors on each side of the differential circuit. The same differential frequency response would result if these grounded capacitors were each replaced by a single differential capacitor across the two circuit halves at one-half the values shown, eliminating the ground connection. There are advantages and drawbacks to each approach. One of the attractions for the implementation of Figure 14 is that this circuit also acts to filter any common-mode signal at high frequencies. Single capacitors across the two circuit halves, on the other hand, will give a wideband, gain of 2 stage for any common-mode input signal or noise. Furthermore, the noise gain shaping capacitors at the inverting inputs need to be grounded separately to correctly implement that noise gain shaping for each amplifier.

This single 5V implementation only requires 10.5mA total supply current (53mW) and gives extremely low distortion and noise. The total load for each amplifier is simply the feedback resistor. This 400Ω load shows approximately 90dBc distortion levels for $2V_{PP}$ in the datasheet plot duplicated in Figure 15. (Ref. 6)

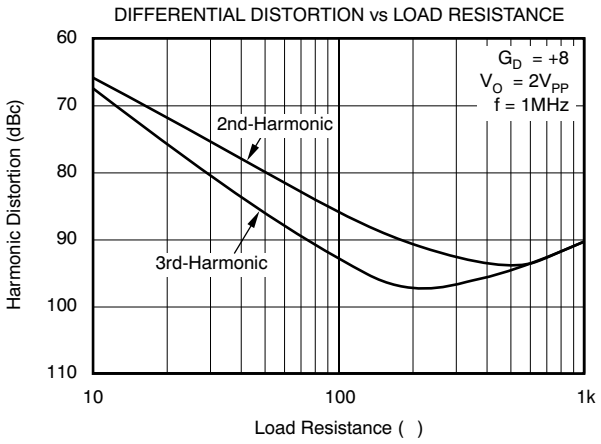

Figure 15. OPA2614 Single +5V Distortion for Noninverting Differential Gain of 8

This distortion improves at the lower noise gain setting used in Figure 14. Going from 8 to 3 should give an approximate 8.5dB improvement from the –95dBc levels shown above to –104dBc. This $2V_{PP}$ differential output is well within the available output voltage swing range. On a single +5V supply, the OPA2614 has a typical 1V headroom requirement to each supply pin. With a $3V_{PP}$ available output on each side, using a +5V supply gives a maximum $6V_{PP}$ differential swing capability. This non-rail-to-rail output stage provides much lower distortion versus quiescent power than rail-to-rail output designs. For higher frequencies and/or even lower distortion in this differential I/O interface, the 1.8GHz gain bandwidth product OPA2846 should be considered.

7 Pole Sensitivity to Amplifier Gain Bandwidth Product

Numerous academic treatments of pole sensitivity functions to filter elements are available (see, for example, Ref. 4). In general, the MFB filter is desirable in that the root loci, as amplifier gain bandwidth reduces, is in the direction of more stability. Specifically, from a starting point of desired pole locations using an infinite bandwidth op amp assumption, the root loci is in the direction of higher ω_o and lower Q as the finite bandwidth amplifiers are inserted into the analysis.

More generally, a single pole model for the op amp can be inserted into the filter transfer function analysis, and then solved for actual pole locations. This process adds a pole to the analysis, making it a 3rd-order transfer function. The general form for that transfer function is shown as Equation 25 with each of the coefficients detailed in Equation 27 through Equation 31. Including the amplifier gain bandwidth product (GBW) complicated the equation significantly in comparison with Equation 1, but essentially moved the actual filter poles slightly and added a real pole at the GBW divided by the high frequency noise gain. Here, no consideration of C_T is being made, but that sets the high frequency real pole added by the real amplifier GBW.

$$\frac{V_O}{V_I} = -\frac{H}{B_3 s^3 + B_2 s^2 + B_1 s + B_0} \tag{25}$$

which uses an op amp single-pole model, given by:

$$A(s) = \frac{A_{OL}\omega_o}{s + \omega_o} \tag{26}$$

Where :

A_{OL} = Open loop gain

$\frac{\omega_o}{2\pi}$ = Dominant pole (Hz)

$\frac{A_{OL}\omega_o}{2\pi}$ = Gain bandwidth product (Hz)

Detailed coefficients for Equation 25 are given below.

$$H = \frac{A_{OL}\omega_o}{C_1C_2R_2R_3} \tag{27}$$

$$B_0 = \frac{\omega_a}{C_1C_2R_1R_2}\left(A_{OL} + 1 + \frac{R_1}{R_2}\right) \tag{28}$$

$$B_1 = \frac{A_{OL}\omega_a}{R_2C_1}\left(1 + \frac{R_2}{R_3 \parallel R_1}\right) + \frac{1 + \frac{R_1}{R_3}}{C_1C_2R_1R_2} + \omega_a\left(\frac{1}{R_2C_2} + \frac{1}{R_2C_1}\left(1 + \frac{R_2}{R_3 \parallel R_1}\right)\right) \tag{29}$$

$$B_2 = (A_{OL} + 1)\omega_a + \omega_a\left(\frac{1}{R_2C_2} + \frac{1}{R_2C_1}\left(1 + \frac{R_2}{R_3 \parallel R_1}\right)\right) \tag{30}$$

$$B_3 = 1 \tag{31}$$

As an example, use this analysis to achieve two different filters using an initial GBW op amp of 220MHz; then step the GBW down in large steps to see the impact on the filter pole locations. Specifically, target a lower frequency Butterworth design; then target a higher frequency, high-Q design. Table 4 steps through the targets and then the actual complex pole locations.

Table 4. Actual Pole Locations vs. Amplifier GBW

OPA GBW (MHz)[1]	Target 200kHz, Q = 0.707		Target 2MHz, Q = 3	
	F_O (kHz)	Q	F_O (MHz)	Q
Infinite (ideal)	200	0.707	2	3
220	200	0.707	2	2.844
139	200	0.706	2	2.76
88	200	0.7055	2.001	2.64
55	200	0.7034	2.003	2.46
35	200	0.7013	2.007	2.23
22	200	0.698	2.017	1.93
14	200	0.693	2.046	1.58
8.8	200.1	0.6845	2.133	1.24

(1) Nominal Gain Bandwidth Product (GBW) = 220MHz.

The lower frequency, low-Q, design can obviously tolerate very slow amplifiers and still hit very near the desired pole locations. The high-Q, higher F_O, design shows very good control over F_O but the Q decreases rapidly with slower amplifiers. Even at 220MHz GBW (100 times over the target F_O), the actual Q is 5% lower than targeted. This is giving what looks like an almost constant ω_o root loci with decreasing angle to the complex poles as they move in a circular path in the s-plane.

Table 4 suggests that the MFB filter is very robust to amplifier bandwidth variations in lower-Q designs. While even a 35MHz GBW does not move the 200kHz, Q = .707 poles very much, higher GBW amplifiers give the higher loop gain discussed earlier, which should lead to lower distortion designs.

Table 4 also points out that higher-Q designs will be very sensitive to the amplifier bandwidth, and thus quite a bit of GBW margin should be provided if a predictable filter response is desired. Additionally, it suggests that to account for the amplifier GBW, simply targeting a higher Q is all that is needed, since the ω_o is not affected as much. Since R_3 is an independent tune for Q (Equation 5), R_3 can be used to *tune in* the Q after a nominal design to account for the finite GBW of the amplifier. The Q equation has a positive derivative to R_3, so increasing R_3 increases the Q if needed (while also decreasing the in-band signal gain) without impacting the ω_o.

For example, do a nominal design for F_O = 5MHz and Q = 1.5 using a 280MHz typical GBW amplifier such as the OPA820, delivering a low frequency gain of –2. Then, include the amplifier GBW in the analysis to find the actual pole locations, re-target Q a bit higher, and re-design the circuit.

Targeting an $R_2 = R_3$ design gives the following filter values, where $R_2 = 350\Omega$ was selected for input noise control:

- R_2 = **350Ω** [selected to control noise using Equation 9]
- C_2 = **12.1pF** [set by targeting $(1 / \omega_o R_2 C_2) = Q(2A_V + 1)$]
- C_1 = **341pF** [set using Equation 10]
- R_3 = **349Ω** [set using Equation B-17]
- R_1 = **700Ω** [set using Equation 2]
- DC Gain (A_V) = **2.00V/V** [from Equation 2]
- F_O = **5MHz** [from Equation 3]
- Q = **1.50** [from Equation 4]

Putting in the actual GBW adds a real pole at 280MHz (recall that the noise gain is 1 at the crossover point for this simple design). We also get the actual complex poles falling at:

- F_O at 5.0004MHz
- Angle = 69.4142°
- Q = 1.4220

The F_O is clearly not affected very much by the amplifier bandwidth, but the Q is quite a bit off. Since the actual Q vs. target Q was a (1.42 / 1.50) = 0.948 ratio, invert this ratio and target the Q at 1.056 times the target.

Retargeting an initial design at Q = 1.58 gives the following solution. In this case, the Q adjustment occurs in the capacitor values since we have separately targeted $R_2 = R_3$ using the analysis shown earlier.

- R_2 = **350Ω** [selected to control noise using Equation 9]
- C_2 = **11.5pF** [set by targeting $(1 / \omega_o R_2 C_2) = Q(2A_V + 1)$]
- C_1 = **359pF** [set using Equation 10]
- R_3 = **349Ω** [set using Equation B-17]
- R_1 = **700Ω** [set using Equation 2]
- DC Gain (A_V) = **2.00V/V** [from Equation 2]
- F_O = **5MHz** [from Equation 3]
- Q = **1.58** [from Equation 4]

Now, including the amplifier bandwidth gives the following complex pole locations (with the same real pole):

- F_O at 5.0004MHz
- Angle = 70.4450°
- Q = 1.4938

This result hits the desired Q very closely and retains the desired gain and F_O targets. This technique is only possible if the designer has a polynomial root finder available to use on the 3rd-order transfer function shown earlier (Equation 25). Nevertheless, this solution does confirm the technique of targeting just a slightly higher Q as the right path to correct pole placement when finite amplifier bandwidth is included in the design. In practice, then, tuning R_3 up slightly from the nominal design (while holding all other components constant) also moves the filter poles towards the desired target (while reducing the gain as well).

8 Summary

The MFB filter is a very desirable filter where excellent stop band rejection is required in a relatively low-Q stage. The methodology developed here gives a means to control the output noise and amplifier loop gain in setting the component values. This approach starts by setting R_2 in Figure 1 to give the same or lower output noise contribution as the op amp itself. This initial step is not necessary for filter implementation, and higher values can be used at the cost of higher output noise. The nature of the MFB filter usually demands widely different capacitor values for implementation. Equal R on the two input resistors (R_3 and R_2 in Figure 1) is, however, a very reasonable design point with the feedback R_1 then set to achieve the desired gain.

For lower-Q designs, setting $R_2 = R_3$ typically places the noise gain zeroes at or above the noise gain poles—thereby limiting unnecessary peaking in the noise gain and its attendant reduction in output dynamic range. Higher-Q designs will suffer from noise gain peaking, both from the zero locations and the desired poles. This effect suggests that the higher-Q designs should be followed by a real pole (RC) and/or set up to cut off well beyond the valid signal frequency range if the lowest distortion is desired. In general, it seems that the MFB filter is more suited to lower-Q filter requirements.

Lower distortion in the MFB filter can be delivered by applying non-unity-gain stable wideband voltage feedback op amps to the design. It is possible to hold the amplifier stable by adding a capacitor on the inverting node in order to shape the noise gain at the crossover point to the needed minimum stable gain value. This adjustment does not affect the desired filter shape, only the noise gain shape at frequencies above the desired filter cutoff. Again, a post-RC filter would be desirable; in this case, to roll off the higher broadband output noise that comes with a noise gain shaped up with frequency.

A design spreadsheet is available to apply the methodology described here using a selection of high-performance op amps. This spreadsheet comprises five related worksheets:

1. **MFBdesign:** this sheet allows the user to select a part number, set target filter specifications, and design the component values. This design sequence has been shown in the examples used in this application note.
2. **PartSelection:** this worksheet contains the list of amplifiers with their required specifications and allows the designer to select a part and then load the needed data in the MFBdesign sheet. The part number must be entered in the MFBdesign sheet exactly as listed here (***note:*** selection is case-sensitive). Also, this sheet shows the resulting loop gain plots and final phase margin. This sheet is where a C_T value would be selected for noise gain control if a non-unity-gain stable amplifier is selected.
3. **NoiseGainPlot:** the noise gain calculations are performed on this worksheet, with the plot replicated in the PartTable sheet.
4. **PartAolgain:** each of the device open-loop gain over frequency values are tabulated
5. **PartAolphase:** each of the device open-loop phase values are tabulated

Note: Within the spreadsheet, designer data entry points are shaded cells with bold format. All other result and data cells are locked to avoid inadvertent data or computation cell changes.

9 References

1. Karki, J. Active low-pass filter design. Texas Instruments application note (SLOA049).
2. Stephens, R. (2004). Active filters using current-feedback amplifiers. Texas Instruments Analog Applications Journal. 2004:3, 21-28.
3. Karki, J. Fully differential amplifiers. Texas Instruments application note (SLOA054).
4. Budak, A. (1974). Passive and active network analysis and synthesis. Boston: Houghton Mifflin. p. 351.
5. FilterPro active filter design application. Texas Instruments software (SBFA001).
6. OPA2614 product datasheet from Texas Instruments (SBOS305).
7. Steffes, M. Noise analysis for high-speed op amps. Texas Instruments application note (SBOA066).

To obtain a copy of the referenced datasheet, software and application reports, visit the Texas Instruments web site at www.ti.com.

Appendix A Output Noise Analysis

Equation A-1 through Equation A-14 develop the solution for the output noise using Figure A-1.

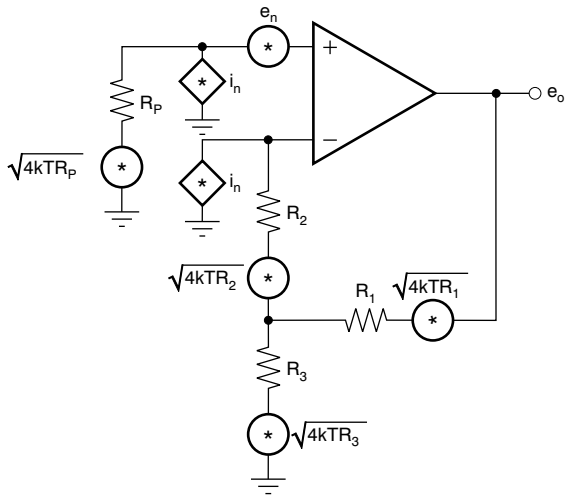

Figure A-1. Noise Analysis Circuit for MFB Filter

Gain for inverting current noise to output (by super-position):

$$e_o = I_n\left(R_2\left(1+\frac{R_1}{R_3}\right)+R_1\right) \tag{A-1}$$

Design constraint to get bias current error cancellation:

$$R_P = R_2 + R_1 \parallel R_3 \tag{A-2}$$

Total output noise by calculating the root mean square (RMS) of each term to the output and then neglecting the R_P terms (assuming it will be bypassed by a large capacitor):

$$e_o = \sqrt{(e_n)^2\left(1+\frac{R_1}{R_3}\right)^2 + 4kTR_2\left(1+\frac{R_1}{R_3}\right)^2 + 4kTR_1\left(1+\frac{R_1}{R_3}\right) + i_n{}^2\left[R_2\left(1+\frac{R_1}{R_3}\right)+R_1\right]^2} \tag{A-3}$$

Set the e_n term equal to the terms arising from R_2 and R_3 (this is dropping out the $[i_n{}^2R_1{}^2]$ term):

$$\left(1+\frac{R_1}{R_3}\right)^2 e_n{}^2 = \left(4kTR_2 + (i_nR_2)^2\right)\left(1+\frac{R_1}{R_3}\right)^2 + i_n{}^2\left(2R_2R_1\left(1+\frac{R_1}{R_3}\right)\right) \tag{A-4}$$

(and Equation 7 in the main text). Because we would like e_n to dominate, we then solve for a limit to R_2:

$$e_n{}^2 \geq 4kTR_2 + (i_nR_2)^2 + i_n{}^2\left[\frac{2R_2R_1}{\left(1+\frac{R_1}{R_3}\right)}\right] \tag{A-5}$$

Solving for equality:

$$e_n{}^2 = 4kTR_2 + i_n{}^2\left(2R_2(R_1 \parallel R_3) + R_2{}^2\right) \tag{A-6}$$

Isolating on R_2 terms:

$$e_n^2 = i_n^2 R_2^2 + R_2\left[4kT + 2i_n^2(R_1 \parallel R_3)\right] \tag{A-7}$$

Then solving for R_2:

$$R_2^2 + R_2\left[\frac{4kT}{i_n^2} + 2(R_1 \parallel R_3)\right] - \left(\frac{e_n}{i_n}\right)^2 = 0 \tag{A-8}$$

Let $R_3 = R_2$ to continue developing an initial limit for a maximum R_2 value.

$$R_2^2 + R_2\left(\frac{4kT}{i_n^2} + \frac{2R_2R_1}{R_2+R_1}\right) - \left(\frac{e_n}{i_n}\right)^2 = 0 \tag{A-9}$$

But:

$$\frac{2R_2R_1}{R_2+R_1} = \frac{2R_2}{1+\frac{R_2}{R_1}} = \frac{2R_2}{1+\frac{1}{A_V}} = \frac{2R_2A_V}{A_V+1} \tag{A-10}$$

where $\frac{R_2}{R_1} = \frac{R_3}{R_1} = \frac{1}{A_V}$ is used (magnitude only, sign not required for noise computations)

.

Then, putting Equation A-10 into Equation A-9:

$$R_2^2 + R_2\left(\frac{4kT}{i_n^2} + \frac{2R_2A_V}{A_V+1}\right) - \left(\frac{e_n}{i_n}\right)^2 = 0 \tag{A-11}$$

Regrouping terms:

$$R_2^2\left(1 + \frac{2A_V}{A_V+1}\right) + R_2\frac{4kT}{(i_n^2)} - \left(\frac{e_n}{i_n}\right)^2 = 0 \tag{A-12}$$

Putting into standard monic form:

$$R_2^2 + R_2\left(\frac{1+A_V}{1+3A_V}\right)\frac{4kT}{(i_n^2)} - \left(\frac{1+A_V}{1+3A_V}\right)\left(\frac{e_n}{i_n}\right)^2 = 0 \tag{A-13}$$

Then, using the quadratic formula, the positive solution for R_2 will be:

$$R_2 = \left(\frac{1+A_V}{1+3A_V}\right)\frac{2kT}{(i_n^2)}\left[\sqrt{1 + \left(\frac{1+3A_V}{1+A_V}\right)\left(\frac{e_n}{2kT}\right)^2} - 1\right] \tag{A-14}$$

This equation (Equation 9 in the text) estimates a maximum R_2 value that will limit the separate noise power contributions of the resistors R_2 and R_3 at the output to approximately equal the op amp input noise voltage contribution.

To achieve this, it assumes that $R_3 = R_2$ and R_P is bypassed by a large capacitor in Figure A-1. In practice, selecting R_2 to be less than the value derived in Equation A-14 and $R_3 < R_2$ would be desirable.

For a background discussion of op amp noise calculations, see Ref. 7.

Appendix B Solution for R_3 and C_1

This appendix, with Equation B-1 through Equation B-21, develops the solution for R_3 and C_1 discussed in this application report, starting from the full filter Laplace transfer function.

$$\frac{V_o}{V_i} = \frac{-1}{C_1C_2R_2R_3} \cdot \frac{1}{s^2 + s\frac{1}{C_1R_2R_3}\left(R_3 + R_2\left(1 + \frac{R_3}{R_1}\right)\right) + \frac{1}{R_1R_2C_1C_2}} \tag{B-1}$$

$$\text{DC Gain}\,(s = 0) = -\frac{R_1}{R_3} \quad \left[\text{define } A_V = \left|-\frac{R_1}{R_3}\right|\right] \quad (\text{We only need gain magnitude for design})$$

$$\omega_o = \sqrt{\frac{1}{R_1R_2C_1C_2}} \tag{B-2}$$

$$Q = \frac{\sqrt{\frac{C_1}{C_2}}}{\sqrt{\frac{R_1}{R_2}} + \sqrt{\frac{R_2}{R_1}} + \frac{\sqrt{R_1R_2}}{R_3}} \qquad [\text{unitless}] \tag{B-3}$$

Define $\alpha \equiv \frac{R_1}{R_2}$:

$$Q = \frac{\sqrt{\frac{C_1}{C_2}}}{\sqrt{\alpha} + \sqrt{\frac{1}{\alpha}} + \frac{\sqrt{\alpha R_2^{\,2}}}{R_3}} \tag{B-4}$$

Simplifying :

$$Q = \frac{R_3\sqrt{\frac{C_1}{C_2}}}{R_3\left(\sqrt{\alpha} + \sqrt{\frac{1}{\alpha}}\right) + R_2\sqrt{\alpha}}$$

$$Q = \frac{R_3\sqrt{\frac{C_1}{C_2}}}{(R_2 + R_3)\sqrt{\alpha} + R_3\left(\frac{1}{\sqrt{\alpha}}\right)} \tag{B-5}$$

Isolating on R_3 :

$$QR_3\left(\sqrt{\alpha} + \sqrt{\frac{1}{\alpha}}\right) + QR_2\sqrt{\alpha} = R_3\sqrt{\frac{C_1}{C_2}}$$

$$R_3\left[\sqrt{\frac{C_1}{C_3}} - Q\left(\sqrt{\alpha} + \sqrt{\frac{1}{\alpha}}\right)\right] = QR_2\sqrt{\alpha}$$

$$R_3 = \frac{QR_2\sqrt{\alpha}}{\sqrt{\frac{C_1}{C_2}} - Q\left(\sqrt{\alpha} + \sqrt{\frac{1}{\alpha}}\right)} = \frac{QR_2}{\sqrt{\frac{C_1}{C_2}}\cdot\frac{1}{\sqrt{\alpha}} - Q\left(1 + \frac{1}{\alpha}\right)} \tag{B-6}$$

Putting $\alpha = \frac{R_1}{R_2}$ back into this :

$$R_3 = \frac{QR_2}{\sqrt{\frac{C_1}{C_2}} \cdot \sqrt{\frac{R_2}{R_1}} - Q\left(1 + \frac{R_2}{R_1}\right)} = \frac{Q}{\sqrt{\frac{C_1}{C_2}} \cdot \sqrt{\frac{1}{R_1R_2}} - \frac{Q}{(R_1 \| R_2)}} \quad \text{(B-7)}$$

Using $\frac{1}{\sqrt{R_1R_2C_1C_2}} = \omega_o$ to get $\frac{1}{\sqrt{R_1R_2}} = \omega_o\sqrt{C_1C_2}$ (B-8)

Substituting this result in :

$$R_3 = \frac{Q}{\sqrt{\frac{C_1}{C_2}}\ \omega_o\sqrt{C_1C_2} - \frac{Q}{(R_1 \| R_2)}} = \frac{Q}{\omega_oC_1 - \frac{Q}{(R_1 \| R_2)}} \quad \text{(B-9)}$$

Multiplying $R_1 \| R_2$ through :

$$R_3 = (R_1 \| R_2)\frac{Q}{\omega_o(R_1 \| R_2)C_1 - Q} \quad \text{(B-10)}$$

Replace $R_1 = A_VR_3$:

$$R_3 = (A_VR_3 \| R_2)\frac{Q}{\omega_o(A_VR_3 \| R_2)C_1 - Q}$$

$$R_3 = \frac{A_VR_3R_2}{A_VR_3 + R_2} \cdot \frac{Q}{\frac{\omega_oA_VR_3R_2C_1}{A_VR_3 + R_2} - Q} \quad \text{(B-11)}$$

Multiply $(A_VR_3 + R_2)$ through denominator :

$$R_3 = \frac{A_VR_3R_2Q}{\omega_oA_VR_3R_2C_1 - Q(A_VR_3 + R_2)} \quad \text{(B-12)}$$

Now divide R_3 out of the numerator to get the right side equal to 1, and then multiply the denominator across:

$$\omega_oC_1(A_VR_3R_2) - QA_VR_3 - QR_2 = A_VR_2Q \quad \text{(B-13)}$$

Isolate and solve for R_3:

$$R_3(\omega_oC_1A_VR_2 - QA_V) = QR_2(A_V + 1) \quad \text{(B-14)}$$

$$R_3 = \frac{QR_2(A_V + 1)}{\omega_oC_1A_VR_2 - QA_V} \quad (\text{one solution for } R_3 \text{ once } C_1 \text{ and } R_2 \text{ are resolved}) \quad \text{(B-15)}$$

Now, to get a second solution for R_3:

Use $\omega_o^2 = \frac{1}{R_1R_2C_1C_2} = \frac{1}{A_VR_3R_2C_1C_2}$ (B-16)

With $R_1 = A_VR_3$ giving $R_3 = \frac{1}{A_V\omega_o^2R_2C_1C_2}$ (B-17)

as a second solution for R_3 to eliminate it for now.

Set the two R_3 equations (Equation B-15 and Equation B-17) equal:

$$R_3 = \frac{1}{A_V\omega_o^2R_2C_1C_2} = \frac{QR_2(A_V + 1)}{\omega_oC_1A_VR_2 - QA_V} \quad \text{(B-18)}$$

Cross−multiply :

$$\omega_o C_1 A_V R_2 - Q A_V = A_V \omega_o^2 R_2^2 C_1 C_2 Q (A_V + 1) \tag{B-19}$$

Isolate on C_1 :

$$Q A_V = C_1 \left(\omega_o A_V R_2 - A_V \omega_o^2 R_2^2 C_2 Q (A_V + 1) \right) \tag{B-20}$$

Pull out $\omega_o A_V R_2$ and solve for C_1:

$$C_1 = \frac{Q A_V}{A_V \omega_o R_2 (1 - \omega_o R_2 C_2 Q (A_V + 1))} \tag{B-21}$$

$$C_1 = \frac{Q}{\omega_o R_2 (1 - Q \omega_o R_2 C_2 (A_V + 1))} \quad \text{(solution for } C_1\text{)} \tag{B-22}$$

which is given as Equation 10 in the text.

With R_2 estimated by the noise analysis, this isolates down to a question of setting the R_2C_2 product. Once the product is set, C_1 is uniquely resolved; then Equation B-15 (or Equation B-17) will give R_3, and then R_1 will be set by the target A_V.

Appendix C Effect of an Equal C Target

This section, by means of Equation C-1 through Equation C-11, develops the solution for $C_1 = C_2$ and its impact on achievable filter response.

Starting from Equation B-22 and constraining $C_1 = C_2$:

$$C_1 = C_2 = \frac{Q}{\omega_o R_2 (1 - R_2 C_2 Q \omega_o (1 + A_V))} \tag{C-1}$$

$$C_2 - C_2^2 (R_2 Q \omega_o (1 + A_V)) = \frac{Q}{\omega_o R_2} \tag{C-2}$$

$$C_2^2 - C_2 \frac{1}{R_2 Q \omega_o (1 + A_V)} + \frac{1}{(R_2 \omega_o)^2 (1 + A_V)} = 0 \tag{C-3}$$

Let: $R_2 \omega_o \sqrt{1 + A_V} = x$ (C-4)

Then:

$$C_2^2 - C_2 \frac{1}{Qx\sqrt{1 + A_V}} + \frac{1}{x^2} = 0 \tag{C-5}$$

In quadratic form:

$$C_2^{\ 2} + bC_2 + c = 0 \tag{C-6}$$

which solves generally as:

$$C_2 = -\frac{b}{2}\left(1 \pm \sqrt{1 - \frac{4c}{b^2}}\right) \tag{C-7}$$

Substituting $b = \frac{-1}{Qx\sqrt{1 + A_V}}$ and $c = \frac{1}{x^2}$,

$$C_2 = \frac{1}{2Qx\sqrt{1 + A_V}} \left(1 \pm \sqrt{1 - \frac{4}{x^2} Q^2 x^2 (1 + A_V)}\right) \tag{C-8}$$

$$C_2 = \frac{1}{2Qx\sqrt{1 + A_V}} \left(1 \pm \sqrt{1 - (2Q)^2 (1 + A_V)}\right) \tag{C-9}$$

Substituting back in from $x = R_2 \omega_o \sqrt{1 + Av}$:

$$C_2 = \frac{1}{2QR_2\omega_o (1 + A_V)} \left(1 \pm \sqrt{1 - (2Q)^2 (1 + A_V)}\right) \tag{C-10}$$

To get non-imaginary solutions for C_2, $(2Q)^2 (1 + A_V) < 1$, letting $A_V = 1$, this solves for 1 at Q = 0.357. At this one solution:

$$C_2 = \frac{1}{2QR_2\omega_o (1 + A_V)} \qquad \text{With } A_V = 1, \text{ this produces } \frac{1}{4QR_2\omega_o} \tag{C-11}$$

Then, with Q = 0.357:

$$C_2 = \frac{1}{1.43 R_2 \omega_o} = C_1 \qquad (\text{if } A_V = 1 \text{ and } Q = 0.357 \text{ is the target}) \tag{C-12}$$

Letting $A_V < 1$ will allow higher Q to be achieved and get $C_1 = C_2$, solving for the radical in Equation C-10, but this is an unlikely design target for an active filter.

Appendix D Noise Gain Zeroes with $C_1 = \infty$

Equation D-1 through Equation D-21 develop the solution for the noise gain zeroes discussed in this application note.

Starting from Equation 18 for the MFB Filter Noise Gain:

$$\frac{1}{\beta} = \frac{s^2 + s\left(\frac{1}{C_1R_3} + \frac{1}{C_1\left(R_1 \| R_2\right)} + \frac{1}{C_2R_2}\right) + \frac{1}{R_2\left(R_1 \| R_3\right)C_1C_2}}{s^2 + s\left(\frac{1}{C_1R_3} + \frac{1}{C_1\left(R_1 \| R_2\right)}\right) + \frac{1}{R_1R_2C_1C_2}} \tag{D-1}$$

The denominator is the desired filter poles. Rewrite this noise gain transfer function in terms of the desired filter shape.

$$\frac{1}{\beta} = \frac{s^2 + s\left(\frac{\omega_o}{Q} + \frac{1}{R_2C_2}\right) + \left(1 + A_V\right)\omega_o{}^2}{s^2 + s\frac{\omega_o}{Q} + \omega_o{}^2} \tag{D-2}$$

to solve for the zero locations.

Define $\frac{\omega_o}{Q} + \frac{1}{R_2C_2} = \frac{\omega_C}{Q_C}$ (D-3)

and substitute: $\omega_o\sqrt{1 + A_V} = \omega_C$ (D-4)

Then the zeroes will be given by the roots of:

$$s^2 + s\frac{\omega_c}{Q_c} + \omega_c{}^2 = 0 \tag{D-5}$$

For $C_1 = \infty$, we know (from Equation 10):

$$\omega_o R_2C_2 = \frac{1}{Q\left(1 + A_V\right)} \tag{D-6}$$

which gives a minimum limit on the Integrator pole:

$$\frac{1}{R_2C_2} = \omega_o Q\left(1 + A_V\right) \tag{D-7}$$

Solve for zero locations if this limit is used to set a boundary on where the zeroes can be placed.

As $(1 / R_2C_2)$ is increased from this minimum value, the linear coefficient for the zeroes polynomial of Equation D-2 will increase. This increase will have the effect of spreading the two zeroes farther apart.

Solving Equation D-5 gives zeroes at:

$$Z_{1,2} = \frac{-\omega_C}{2Q_C}\left(1 \pm \sqrt{1-(2Q_C)^2}\right) \tag{D-8}$$

Let $\omega_C = \omega_o\sqrt{1+A_V}$ and setting Q_C to have $\frac{1}{R_2C_2} = \omega_o Q(1+A_V)$

$$Q_C = \frac{\omega_c}{\frac{\omega_o}{Q} + \frac{1}{R_2C_2}} = \frac{\omega_o\sqrt{1+A_V}}{\frac{\omega_o}{Q} + \omega_o Q(1+A_V)} = \frac{Q\sqrt{1+A_V}}{1+Q^2(1+A_V)} \tag{D-9}$$

Substituting these into zero Equation D-8 gives:

$$Z_{1,2} = \frac{-\frac{\omega_o\sqrt{1+A_V}}{2Q\sqrt{1+A_V}}}{1+Q^2(1+A_V)}\left[1 \pm \sqrt{1-\left[\frac{2Q\sqrt{1+A_V}}{1+Q^2(1+A_V)}\right]^2}\right] \tag{D-10}$$

Simplifying:

$$Z_{1,2} = -\frac{\omega_o}{2Q}\left(1+Q^2(1+A_V)\right)\left[1 \pm \sqrt{1-\frac{4Q^2(1+A_V)}{\left(1+Q^2(1+A_V)\right)^2}}\right] \tag{D-11}$$

Define $x = Q\sqrt{1+A_V}$ to substitute in temporarily. (D-12)

This gives zeroes at:

$$Z_{1,2} = \frac{-\omega_o}{Q}\left(\frac{1+x^2}{2}\right)\left[1 \pm \sqrt{1-\frac{4x^2}{(1+x^2)^2}}\right] \tag{D-13}$$

Distribute $\frac{1+x^2}{2}$ through :

$$Z_{1,2} = \frac{-\omega_o}{Q}\left[\frac{1+x^2}{2} \pm \sqrt{\left(\frac{1+x^2}{2}\right)^2 - x^2}\right] \tag{D-14}$$

Expand terms in the radical:

$$Z_{1,2} = \frac{-\omega_o}{Q}\left[\frac{1+x^2}{2} \pm \sqrt{\frac{1}{4}+\frac{x^2}{2}+\frac{x^4}{4}-x^2}\right] \tag{D-15}$$

$$Z_{1,2} = \frac{-\omega_o}{Q}\left[\frac{1+x^2}{2} \pm \frac{1}{2}\sqrt{1-2x^2+x^4}\right] = \frac{-\omega_o}{Q}\left[\frac{1+x^2}{2} \pm \frac{1}{2}\sqrt{(x^2-1)^2}\right] \tag{D-16}$$

$$Z_{1,2} = \frac{-\omega_o}{Q}\left[\frac{1}{2}+\frac{x^2}{2} \pm \left(\frac{x^2}{2}-\frac{1}{2}\right)\right] \tag{D-17}$$

Solving for each zero and substituting back in for x:

$$Z_1 = \frac{-\omega_o}{Q}\left[x^2\right] = \frac{-\omega_o}{Q}Q^2(1+A_V) = -\omega_o Q(1+A_V) \quad \text{(D-18)}$$

$$Z_2 = \frac{-\omega_o}{Q}[1] = \frac{-\omega_o}{Q} \qquad \left[\text{if } Q > 1, \ |Z_2| < \omega_o\right] \quad \text{(D-19)}$$

To get repeated real zeroes, set $Z_1 = Z_2$ and solve :

$$\frac{\omega_o}{Q} = \omega_o Q(1+A_V)$$

$$\text{or when: } 1 = Q^2(1+A_V) \quad \text{(D-20)}$$

For instance, Q = 0.707 and A_V = 1 will give repeated zeroes at:

$$Z_1 = Z_2 = -\omega_o\sqrt{2} \quad \text{(D-21)}$$

This analysis shows that at the limit—where C_1 solves for infinity by setting ($[1 / R_2C_2] = \omega_o Q [1 + A_V]$)—and the very common filter target of a Butterworth filter at a gain of 1, this filter has noise gain zeroes that are repeated and that fall at ($\sqrt{2}\ \omega_o$) which is well beyond the filter poles. Moving the Integrator pole up ($1 / R_2C_2$) to get real solutions for C_1 will be splitting these two zeroes, with one coming down in frequency and the other moving up in frequency.

Appendix E Noise Gain Zeroes for $R_3 = R_2$ Targeted

Equation E-1 through Equation E-21 develop the solution for the noise gain zeroes if $R_3 = R_2$ is desired.

Start with the solution for R_3 from Equation B-15.

$$R_3 = \frac{QR_2(A_V+1)}{\omega_o A_V R_2 C_1 - QA_V} \tag{E-1}$$

Substitute in for C_1 from Equation B-22:

$$C_1 = \frac{Q}{\omega_o R_2(1-Q\omega_o R_2 C_2(A_V+1))} \tag{E-2}$$

$$R_3 = \frac{QR_2(A_V+1)}{\frac{\omega_o A_V R_2 Q}{\omega_o R_2(1-Q\omega_o R_2 C_2(A_V+1))} - QA_V} \tag{E-3}$$

Pulling $\frac{A_V+1}{A_V}$ out and cancelling Q, dividing $\omega_O R_2$ out of the first denominator term :

$$R_3 = \frac{A_V+1}{A_V}\frac{R_2}{\frac{1}{(1-Q\omega_o R_2 C_2(A_V+1))} - 1} \tag{E-4}$$

Multiplying the denominator term through :

$$R_3 = \frac{A_V+1}{A_V}R_2\frac{1-Q\omega_o R_2 C_2(A_V+1)}{1-1+Q\omega_o R_2 C_2(A_V+1)} = \frac{A_V+1}{A_V}R_2\left[\frac{1}{Q\omega_o R_2 C_2(A_V+1)} - 1\right] \tag{E-5}$$

$$R_3 = \frac{1}{Q\omega_o C_2 A_V} - \frac{A_V+1}{A_V}R_2 = \frac{R_2}{Q\omega_o R_2 C_2 A_V} - R_2\left(1+\frac{1}{A_V}\right) \tag{E-6}$$

Set $R_3 = R_2$ and solve the resulting expression for $\omega_o R_2 C_2$:

$$R_2 = R_2\left[\frac{1}{Q\omega_o R_2 C_2 A_V} - 1 - \frac{1}{A_V}\right] \tag{E-7}$$

$$1 = \frac{1}{Q\omega_o R_2 C_2 A_V} - 1 - \frac{1}{A_V} \tag{E-8}$$

$$2 = \frac{1}{A_V}\left(\frac{1}{Q\omega_o R_2 C_2} - 1\right) \tag{E-9}$$

$$\text{then } 2A_V+1 = \frac{1}{Q\omega_o R_2 C_2} \tag{E-10}$$

$$\omega_o R_2 C_2 = \frac{1}{Q(2A_V+1)} \tag{E-11}$$

or:

$$\frac{1}{\omega_o R_2 C_2} = Q(2A_V+1)$$

Setting $\omega_o R_2 C_2$ to this value in Equation E-2 will give a valid C_1 solution. Now go on to solve for the zero location if $(1 / R_2 C_2) = \omega_o Q(2A_V + 1)$ in Equation D-2.

Now go back to the zero equation (from Equation D-8):

$$Z_{1,2} = -\frac{\omega_C}{2Q_C}\left(1 \pm \sqrt{1-(2Q_C)^2}\right) \text{ where :} \tag{E-12}$$

$$\omega_C = \omega_o\sqrt{1+A_V}$$

and

$$Q_C = \frac{\omega_c}{\frac{\omega_o}{Q} + \frac{1}{R_2C_2}}$$

Then, putting in $\frac{1}{R_2C_2} = \omega_o Q(2A_V+1)$: (E-13)

which will be forcing $R_3 = R_2$,

$$Q_C = \frac{\omega_o\sqrt{1+A_V}}{\frac{\omega_o}{Q} + \omega_o Q\left(2A_V+1\right)} = \frac{Q\sqrt{1+A_V}}{1+Q^2(2A_V+1)} \tag{E-14}$$

Then, going back to $Z_{1,2}$ (Equation E-12) and substituting in:

$$Z_{1,2} = \frac{-\omega_o\sqrt{1+A_V}}{\frac{2Q\sqrt{1+A_V}}{1+Q^2\left(2A_V+1\right)}}\left[1 \pm \sqrt{1-\left[\frac{2Q\sqrt{1+A_V}}{1+Q^2\left(2A_V+1\right)}\right]^2}\right] \tag{E-15}$$

$$Z_{1,2} = -\frac{\omega_o}{2Q}\left(1+Q^2\left(2A_V+1\right)\right)\left[1 \pm \sqrt{1-\left[\frac{2Q\sqrt{1+A_V}}{1+Q^2\left(2A_V+1\right)}\right]^2}\right] \tag{E-16}$$

These will be noise gain zeroes with: $\omega_o R_2C_2 = \frac{1}{Q(2A_V+1)}$ (E-17)

which will constrain: $R_3 = R_2$ (E-18)

So, in general: $\frac{1}{Q(2A_V+1)} \le \omega_o R_C C_2 < \frac{1}{Q(A_V+1)}$ (E-19)

with $\frac{1}{Q(2A_V+1)}$ derived via $R_3 = R_2$ *and* $\frac{1}{Q(A_V+1)}$ derived via $C_1 \to \infty$. (E-20)

It is a bit easier to write the constraint in inverted form. This becomes the ratio of the Integrator pole ($1 / R_2C_2$) to the desired filter ω_o.

$$Q(2A_V + 1) \quad \frac{1}{{}_oR_2C_2} > Q(A_V + 1)$$

$R_3 = R_2$ limit $\qquad$ $C_1 =$ limit (E-21)

IMPORTANT NOTICE

Texas Instruments Incorporated and its subsidiaries (TI) reserve the right to make corrections, modifications, enhancements, improvements, and other changes to its products and services at any time and to discontinue any product or service without notice. Customers should obtain the latest relevant information before placing orders and should verify that such information is current and complete. All products are sold subject to TI's terms and conditions of sale supplied at the time of order acknowledgment.

TI warrants performance of its hardware products to the specifications applicable at the time of sale in accordance with TI's standard warranty. Testing and other quality control techniques are used to the extent TI deems necessary to support this warranty. Except where mandated by government requirements, testing of all parameters of each product is not necessarily performed.

TI assumes no liability for applications assistance or customer product design. Customers are responsible for their products and applications using TI components. To minimize the risks associated with customer products and applications, customers should provide adequate design and operating safeguards.

TI does not warrant or represent that any license, either express or implied, is granted under any TI patent right, copyright, mask work right, or other TI intellectual property right relating to any combination, machine, or process in which TI products or services are used. Information published by TI regarding third-party products or services does not constitute a license from TI to use such products or services or a warranty or endorsement thereof. Use of such information may require a license from a third party under the patents or other intellectual property of the third party, or a license from TI under the patents or other intellectual property of TI.

Reproduction of information in TI data books or data sheets is permissible only if reproduction is without alteration and is accompanied by all associated warranties, conditions, limitations, and notices. Reproduction of this information with alteration is an unfair and deceptive business practice. TI is not responsible or liable for such altered documentation.

Resale of TI products or services with statements different from or beyond the parameters stated by TI for that product or service voids all express and any implied warranties for the associated TI product or service and is an unfair and deceptive business practice. TI is not responsible or liable for any such statements.

Following are URLs where you can obtain information on other Texas Instruments products and application solutions:

Products		**Applications**	
Amplifiers	amplifier.ti.com	Audio	www.ti.com/audio
Data Converters	dataconverter.ti.com	Automotive	www.ti.com/automotive
DSP	dsp.ti.com	Broadband	www.ti.com/broadband
Interface	interface.ti.com	Digital Control	www.ti.com/digitalcontrol
Logic	logic.ti.com	Military	www.ti.com/military
Power Mgmt	power.ti.com	Optical Networking	www.ti.com/opticalnetwork
Microcontrollers	microcontroller.ti.com	Security	www.ti.com/security
		Telephony	www.ti.com/telephony
		Video & Imaging	www.ti.com/video
		Wireless	www.ti.com/wireless

Mailing Address: Texas Instruments
Post Office Box 655303 Dallas, Texas 75265